RHEUMATOLOGY

Rheumatology 2019;58:1777–1783
doi:10.1093/rheumatology/kez130
Advance Access publication 16 April 2019

Concise report

The simultaneous analysis of mesenchymal stem cells and early osteocytes accumulation in osteoarthritic femoral head sclerotic bone

Dragos C. Ilas [1], Sarah M. Churchman [1], Thomas Baboolal [1], Peter V. Giannoudis [1], Joseph Aderinto [2], Dennis McGonagle [1] and Elena Jones [1]

Abstract

Objective. OA subchondral bone is a key target for therapy development. Osteocytes, the most abundant bone cell, critically regulate bone formation and resorption. Their progenitors, mesenchymal stem cells (MSCs), display altered behaviour in osteoarthritic subchondral bone. This study investigated the relationships between native osteocytes and native MSCs in osteoarthritic femoral heads.

Methods. To avoid culture manipulations, a bone treatment procedure was developed to simultaneously obtain pure osteocyte-enriched fragments and matched native $CD45^{-}CD271^{+}$ MSCs. Gene expression in osteocytes and MSCs was compared between healthy and OA bone and selected molecules were examined by immunohistochemistry in relation to OA tissue pathology. Cell sorting and standard trilineage differentiation assays were employed to test OA MSC functionality.

Results. Native osteocyte enrichment was confirmed histologically and by higher-level osteocyte maturation transcripts expression, compared with purified MSCs. Compared with healthy bone, native OA osteocytes expressed 9- and 4-fold more early/embedding osteocyte molecules E11 and MMP14, and 6-fold more osteoprotegerin ($P<0.01$). $CD271^{+}$ MSCs accumulated in the regions of bone sclerosis (9-fold, $P<0.0001$) in close juxtaposition to trabeculae densely populated with morphologically immature E11-positive osteocytes (medians of 76% *vs* 15% in non-sclerotic areas, $P<0.0001$), and osteoblasts. Gene expression of OA MSCs indicated their bone formation bias, with retained multipotentiality following culture-expansion.

Conclusions. In human late-stage OA, osteogenically-committed MSCs and adjacent immature osteocytes exhibit a marked accumulation in sclerotic areas. This hitherto unappreciated MSC-early osteocyte axis could be key to understanding bone abnormalities in OA and represents a potential target for novel therapy development in early disease.

Key words: OA, hip, bone, mesenchymal stem cells, osteocytes

Rheumatology key messages

- Accumulation of both early-osteocytes and mesenchymal stem cells in hip OA bone sclerotic areas.
- Native OA mesenchymal stem cells and osteocytes gene expression favours bone formation and inhibition of bone resorption.
- This ‘early-osteocyte – mesenchymal stem cell axis’ offers novel mechanistic explanation for hip OA subchondral bone sclerosis.

Introduction

OA is a disease of the whole joint characterized by pathological changes to cartilage, subchondral bone (SB) and other joint structures [1, 2]. Irrespective of the site of initiation, SB sclerosis is an important feature in OA pathophysiology [3]. Other significant alterations include cysts, emergence of osteophytes and changes in bone remodelling activity [4]. Of even greater importance, MRI studies have shown that subchondral MRI-determined bone marrow lesions are associated with rapid OA progression [5], underscoring the crucial role of SB pathology in OA pathogenesis [2, 4].

Osteocytes are by far the most abundant bone cells and are now recognized as master regulators of the bone remodelling cascade [6]. However, most studies have

[1]Leeds Institute of Rheumatic and Musculoskeletal Medicine, The University of Leeds and [2]Department of Orthopaedics, Chapel Allerton, Leeds Teaching Hospitals NHS Trust, Leeds, UK

Submitted 23 October 2018; accepted 13 March 2019

Correspondence to: Elena Jones, Leeds Institute of Rheumatic and Musculoskeletal Medicine, Room 5.23 Clinical Sciences Building, St James’s University Hospital, Leeds LS9 7TF, UK.
E-mail: e.jones@leeds.ac.uk

CLINICAL SCIENCE

focused on the bone remodelling process and its chief participant cells, osteoblasts and osteoclasts [7]. To better understand the cellular mechanisms behind SB changes in OA, further elucidation of other bone-lineage cells, including the earliest osteoblast progenitors, mesenchymal stem cells (MSCs), or their terminally-differentiated descendants, osteocytes, is needed.

We recently documented an increase in the MSC numbers in bone marrow lesion regions of OA femoral heads where they accumulated in the areas of cartilage damage and bone sclerosis. However, these MSCs had a poorer *in vitro* mineralisation capacity and altered expression of key bone remodelling molecules, RANKL and osteoprotegerin (OPG) [8]. We hypothesized that these characteristics propagate to their differentiated progeny (including osteocytes) and therefore have a broader impact on the remodelling activity in OA bone. In support of this, high density of viable osteocytes has been recently described in knee OA bone marrow lesions [9].

To address this, we first developed a method for the simultaneous analysis of MSCs and osteocytes in human bone without the need for culture manipulations. As osteocyte remodelling activity depends on its stage of maturation, we selected a panel of genes spanning early to late osteocyte markers (e.g. podoplanin/E11 [10] and sclerostin (SOST) [11] respectively) as well as those specific to MSCs [12]. Having discovered an early-osteocyte transcript upregulation in OA bone, we hypothesized that it could be related to new bone formation in OA and therefore investigated topographic relationships between native MSCs and osteocytes in OA femoral heads in relation to disease-associated pathology. Herein, we report a significant increase in early-embedding osteocytes adjacent to MSCs in the regions of sclerosis in OA bone. These data implicate atypical MSC accumulation and dysregulated differentiation as potentially major contributors to SB pathology, and hence a potential therapeutic target for disease modification in hip OA.

Methods

Sample processing, gene expression and tripotentiality analysis

This research was undertaken after approval from the Leeds East National Research Ethic Committee and informed written consent was obtained from all patients and healthy donors enrolled in the study. Femoral heads were obtained from patients undergoing total hip arthroplasty for primary OA ($n = 26$). Healthy iliac crest (IC) bone ($n = 11$) and femoral heads from fragility neck of femur fracture (NFF) patients ($n = 3$) were used as controls. Iliac crest biopsies were collected from patients undergoing orthopaedic surgery for metal removal following previous fracture, who were otherwise healthy. All bone samples were collected and processed on the day of the surgery and are detailed in the Supplementary Table S1, available at *Rheumatology* online. Bone-resident MSCs were extracted by 4-h enzymatic digestion [8] and cell sorting [12, 13]. Following digestion, the bone fragments were rigorously washed four times in large volumes of PBS using a method modified from Pathak *et al*. [14] to remove all residual cellular material from the bone surface. Osteocyte-enriched bone fragments were next homogenized in lysis buffer (guanidine isothiocyanate solution with 0.4% sodium citrate, 1% N-lauryl sarcosine and 0.5% β-mercaptoethanol) and RNA was precipitated with isopropanol and DNase treated (Invitrogen, Fisher Scientific, Leicestershire, UK). Total RNA from FACS-purified $CD45^-CD271^+$ MSCs and control $CD45^+CD271^-$ haematopoietic-lineage cells [12] was extracted using the Single-Cell RNA Extraction kit (Norgen Biotek, Geneflow, Lichfield, UK) and on-column DNase (Applied Biosystems, Foster City, California, USA) treated. cDNA was synthesized using the High-Capacity cDNA Reverse Transcription Kit (Applied Biosystems, Foster City, California, USA). qPCR was performed on a QuantStudio7Flex Real-Time PCR System (Applied Biosystems) and gene expression levels normalized relative to housekeeping gene *HPRT1*. The TaqMan probes for the genes of interest are detailed in Supplementary Table S2, available at *Rheumatology* online, all from Thermo Fisher. To evaluate multipotentiality, FACS-purified $CD45^-CD271^+$ were culture-expanded and differentiated towards osteogenic, adipogenic and chondrogenic lineages as described previously [8, 12].

Histology and immunohistochemistry

Whole femoral heads and IC bone fragments were fixed in 4% paraformaldehyde before decalcifying in EDTA (0.5 M, pH 7.4, Sigma, Dorset, UK). Sections (5μm) were deparaffinized in Xylene (Sigma) and rehydrated in graded ethanol before staining with Haematoxylin-eosin and Safranin O using standard protocols. Immunohistochemistry was performed using the EnVision$^+$Dual Link System-HRP (DAB+) kit (DAKO, Agilent Technologies, Stockport, UK) following manufacturer's instructions. Briefly, the endogenous peroxidase activity was blocked by 10 min incubation with dual enzyme blocking solution (DAKO kit) then the tissues were incubated with primary antibodies against CD271 (1: 100, clone NGFR5, Abcam), E11 (1: 200, clone NZ1, Merck Millipore, Millipore, Watford, UK) and OPG (1: 500, polyclonal, Abcam) for 1 h at room temperature followed by the secondary reagent, Labelled polymer-HRP (DAKO kit) for 30 min at room temperature. Visualisation was achieved by incubation with 3-diaminobenzidine (DAB, DAKO kit) and counterstained with Harris haematoxylin and Scott's water substitute (both from Sigma). Bone area measurements and antibody staining were quantified using Nuance Multispectral Imaging System (Calliper) in selected regions differing in degrees of OA bone pathology (sclerotic, S and non-sclerotic, NS). Semi-automatic counting of E11-positive osteocytes and CD271-positive MSCs was performed within a defined bone or bone cavity area, respectively, using a minimum 10 regions per patient.

The statistical analyses were performed using Mann–Whitney test for comparisons between two groups, Kruskal-Wallis analysis for the intergroup differences, corrected with the Bonferroni-Dunn multiple-

group comparison and Friedman test for the donor matched samples.

Results

Differential gene expression between osteocytes and MSCs in healthy and OA bone

To investigate the gene expression profiles of native human osteocytes compared with their MSC progenitors, a protocol for the simultaneous preparation of osteocyte-enriched bone and uncultured MSCs from the same bone was developed. Haematoxylin-eosin stained trabecular bone before enzymatic treatment showed bony trabeculae covered by bone-lining cells surrounding the highly cellular bone marrow (Fig. 1A). Following collagenase treatment and extensive PBS washes, the stromal tissue and bone-lining cells were completely removed leaving only embedded osteocytes as the remaining cellular material (Fig. 1A). Osteocyte and MSC identified following the above procedure were investigated by comparing their gene expression with donor-matched haematopoietic-lineage cells (a non-mesenchymal lineage population) as control.

The classic markers of osteocyte maturation (*SOST*, *DMP1, MEPE* and *PHEX*) [11] were significantly higher in osteocyte-enriched bone compared with MSCs, confirming a more mature differentiation stage of embedded osteocytes. Molecules associated with early osteocyte development [11] DKK1, E11 and MMP14 did not show the same pattern of higher expression in osteocytes compared with MSCs (Fig. 1B). In contrast, *CXCL12*, a highly-expressed molecule characteristic of MSC stromal support activity, early-osteoblast lineage molecules *SP7* (osterix) and alkaline phosphatase (*ALPL*) were expressed at higher levels in MSCs (Fig. 1B). This differential gene expression pattern taken together with the histological assessment confirmed osteocyte enrichment following our bone processing protocol, which was next used to compare osteocyte gene expression between healthy and OA bone.

No significant differences in the expression of osteocyte-specific molecules were noted between healthy and OA osteocytes, apart from the early/embedding osteocyte markers *E11* and *MMP14,* which were 9-fold (P =0.0028) and 4-fold (P =0.0097) higher in OA, respectively (Fig. 1C). *RANKL* expression showed no significant difference between healthy and OA bone osteocytes, whereas *OPG* expression levels were 6-fold higher in OA (P =0.0033, Fig. 1C). In comparison to NFF, similar elevated levels of *E11*, *MMP14* and *OPG* were observed in OA osteocytes, while no change was observed in *RANKL* levels of mRNA (Fig. 1C). This indicated that the altered osteocytes gene expression is OA specific and not related to weight-bearing sites. Supplementary Table S3, available at *Rheumatology* online, illustrates raw gene expression data for experiments presented in Fig. 1B and C.

Taken together, these patterns of expression suggested higher early-osteocyte activity and a potential contribution for inhibition of bone resorption by osteocytes resident in OA femoral head bone.

Osteocyte and MSC distribution in relation to bone pathology in OA

To investigate if expression of early-osteocyte genes in OA bone reflected active osteocyte formation process, the distribution of CD271-positive MSCs and E11-positive osteocytes was analysed on whole sections of OA femoral heads and compared between sclerotic and NS regions (Fig. 2A), as well as control IC and NFF bone (Supplementary Fig. S1, available at *Rheumatology* online). NS regions in OA, similarly to IC bone were characterized by significantly lower percentage area occupied by bone tissue compared with sclerotic regions of OA femoral heads (averages of 18% and 63%, respectively, P <0.0001, Fig. 2A).

In sclerotic regions, CD271-positive MSCs were highly abundant in the fibrovascular tissue that had replaced bone marrow and/or breached the tidemark, with the highest density of positive cells present around blood vessels and near bone surfaces lined with cuboidal osteoblasts (Fig. 2B), which were negative for CD271 (Supplementary Fig. S2A, available at *Rheumatology* online). The area of CD271 positivity was significantly greater (9-fold, P <0.0001) in sclerotic regions compared with NS regions (Fig. 2C), where CD271-positive cell frequency and distribution was similar to healthy IC and NFF bone (Supplementary Fig. S1, available at *Rheumatology* online).

Early-osteocyte marker E11-positive staining was found in osteocytes near the outer edges of thick trabeculae in sclerotic regions, with the highest density proximal to cuboidal osteoblasts (Fig. 2B), consistent with them being newly embedding in bone [11]. These osteocytes had a distinct morphology with disorganized dendritic processes (Fig. 2C). In contrast, E11-positive osteocytes in NS regions had an elongated shape with more aligned dendritic processes and were significantly (5-fold, P <0.0001) less numerous (Fig. 2C), consistent with IC and NFF bone (Supplementary Fig. S1, available at *Rheumatology* online).

Strong OPG staining was most notable through the entire fibrovascular tissue, osteoblasts and some osteocytes (Fig. 2B). In NS areas, much weaker OPG staining was observed in rare osteocytes and stromal cells, similar to IC and NFF bone (Supplementary Fig. S1, available at *Rheumatology* online).

Altered gene expression profile of CD45-CD271+ MSCs in OA bone

To investigate if MSC/early osteocyte co-localisation could be a result of skewed differentiation of MSCs towards osteogenesis, $CD45^{-}CD271^{+}$ MSCs purified from healthy and OA bone were compared for expression of genes indicative of MSC multipotentiality (Fig. 2D). Using this phenotype, osteoblasts and osteoclasts were excluded from the sorting gate, confirmed by immunohistochemistry (Supplementary Fig. S2A and B, available at

FIG. 1 Gene expression in OCY, CD45$^-$CD271$^+$ MSCs and CD45$^+$CD271$^-$ HLCs from OA and control bone

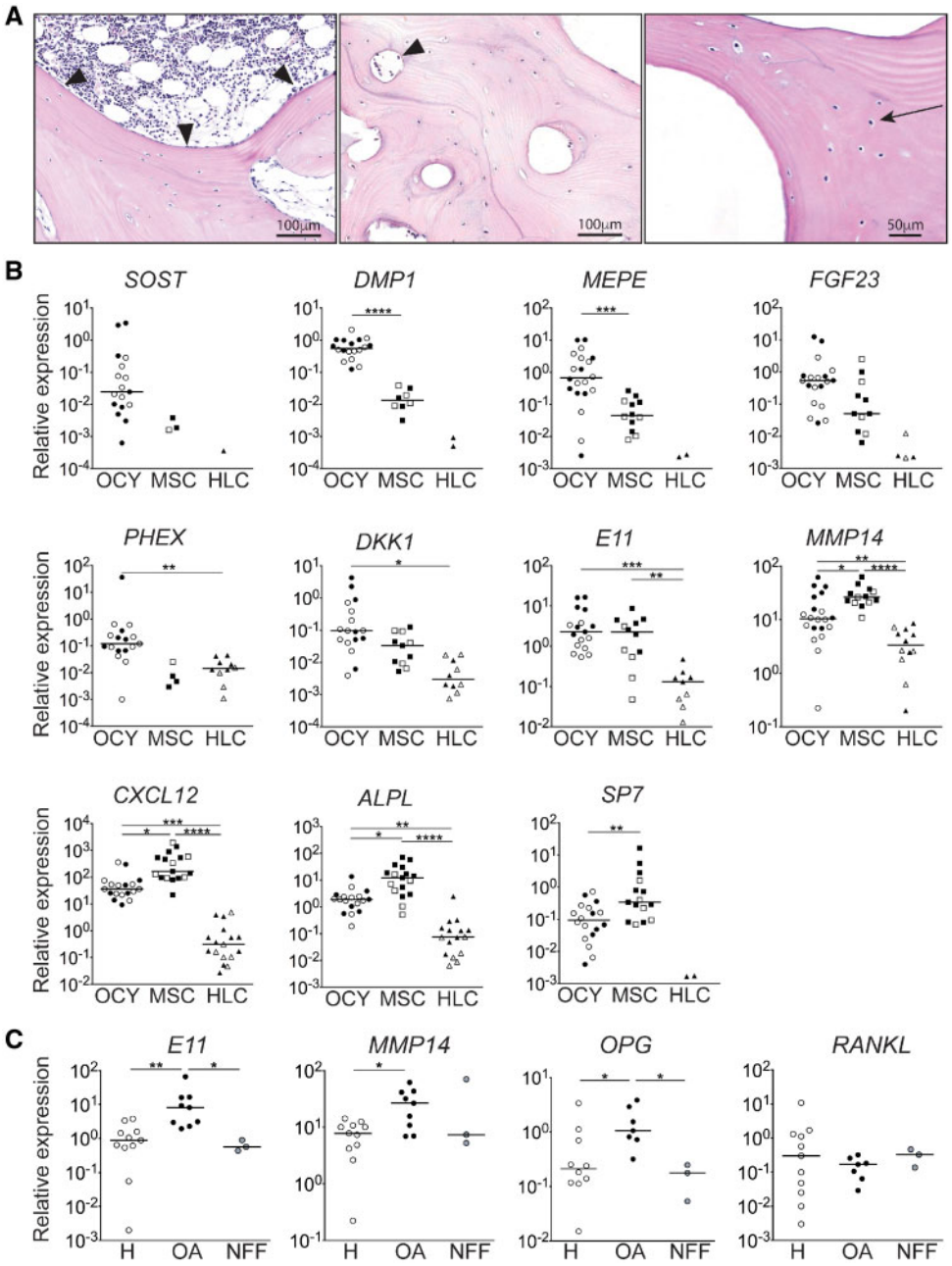

(**A**) Generation of osteocyte-enriched bone: tissue before any treatment (left panel), minimal cells remaining in deep pores after enzymatic digestion and two PBS washes (middle panel) and complete removal of residual bone lining cells following final two washes (right panel). Arrows: osteocytes; arrowheads: bone-lining cells. (**B**) Osteocyte- and MSC/early osteoblast-specific gene expression in OCY (n=20), MSCs (n=17) and HLCs (n=17) from healthy (empty symbols) and OA (filled symbols) bone; the missing dots for some osteocytes transcripts in MSCs and HLCs indicate below detection values in those cell types, precluding full statistical analysis of these data sets. (**C**) Gene expression in osteocytes from bone of healthy (H, empty symbols), OA (black symbols) and NFF donors (NFF, grey symbols). Data presented as dots with median values on logarithmic scale relative to HPRT1. *P <0.05, **P <0.01, ***P <0.001, ****P <0.0001, Kruskal-Wallis analysis for intergroup differences, corrected with Bonferroni-Dunn multiple-group comparison. NFF: neck of femur fracture; HLC: haematopoietic-lineage cells; MSC: mesenchymal stem cells; OCY: osteocytes.

Fig. 2 Pathological features of MSCs and osteocytes in OA femoral heads

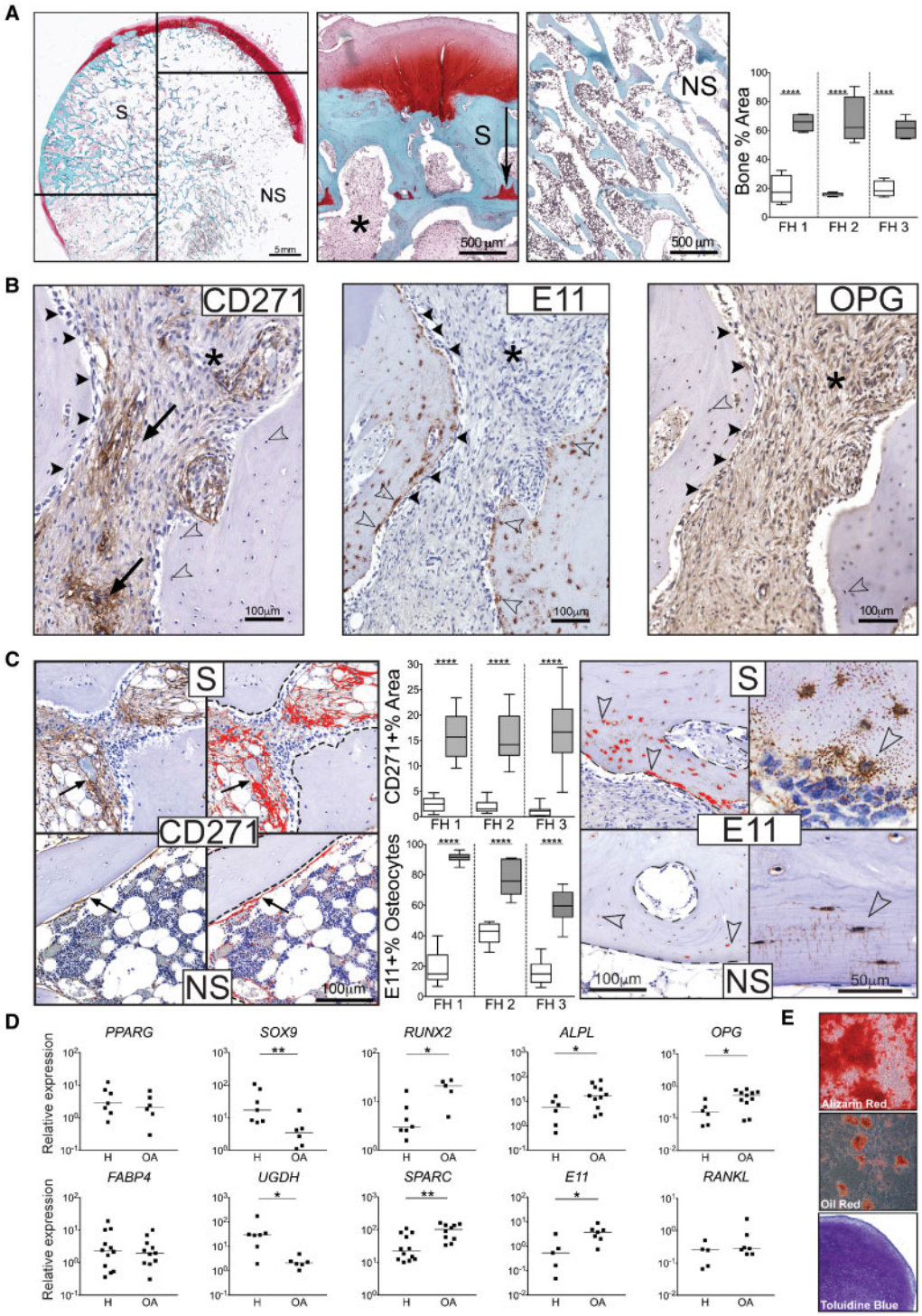

(**A**) Safranin O staining of OA FH showing S and NS regions used for IHC and percentages of bone area occupied in FH from three OA donors (empty boxes: NS; grey boxes: S regions); arrow: remaining area of tidemark. (**B**) Abundance of $CD271^{+}$cells in S regions dominated by OPG^{+} dense fibrovascular tissue (indicated as *) adjacent to $E11^{+}$ osteocytes. (**C**) High-magnification images of CD271 and E11 IHC in S (upper panels) and NS (lower panels) regions of OA FHs and quantification of CD271-stained area and proportions of $E11^{+}$ osteocytes. CD271 area and E11 quantification was performed based on DAB+ staining (brown), within selected bone areas (dashed lines) above negative control threshold (red colour). (**D**) Gene expression in sorted $CD45^{-}CD271^{+}$MSCs from healthy and OA bone. $^{*}P < 0.05$; $^{**}P < 0.01$; $^{****}P < 0.0001$. (**E**) Tri-lineage differentiation ability of OA $CD45^{-}CD271^{+}$ MSCs following culture-expansion. Empty arrow heads: $E11^{+}$ osteocytes; full arrow heads: osteoblasts; arrow: $CD271^{+}$MSCs. FH: femoral head; S: sclerotic; NS: non-sclerotic; IHC: immunohistochemistry; DAB: diaminobenzidine.

Rheumatology online). While the expression of fat-lineage transcripts *PPARγ* and *FABP4* was unaltered in OA MSCs, the chondrogenic transcription factor *SOX9* as well as *UGDH* (UDP-glucose dehydrogenase), involved in glycosaminoglycans biosynthesis, were downregulated (5-fold, P =0.0082 and 14-fold, P =0.0140, respectively). Bone-lineage transcripts *RUNX2, ALPL* and *SPARC* (osteonectin) as well as *E11* were significantly upregulated (P <0.05 for all); while the *OPG,* but not *RANKL* levels were increased. Following culture expansion, sorted $CD45^{-}CD271^{+}$ OA MSCs retained their ability for tri-lineage differentiation (Fig. 2E).

Discussion

Whereas previous studies have reported on the death of osteocytes in OA [9, 15], this study documents an increase in immature osteocytes, specifically in regions of active bone formation and MSC accumulation in OA bone. It also shows that compared with healthy IC bone, OA MSCs displayed a gene expression pattern indicative of preferential osteogenic commitment including an elevated expression of osteoblast-osteocyte transition molecule E11 and resorption-inhibitor OPG. These findings indicate that atypical MSC accumulation and their preferential osteogenic differentiation, previously documented in OA animal models [16] also occur in humans, which may directly contribute to bone sclerosis in hip OA.

Osteocytes are key mechanosensitive cells, which sense and transmit biomechanical signals through a highly interconnected network of finely-organized dendritic processes [6]. As such, they may be involved in both initiation and propagation of OA [15–17]. Early E11-positive osteocytes found in the outer edges of thickened trabeculae in areas of bone sclerosis and cartilage loss, in the present study had disorganized dendritic processes. Given a recently discovered role of E11 in regulating bone modelling/remodelling [18, 19], this suggests a reduction in mechanosensing capabilities of this newly formed bone, which may further impact on the quality of the remaining articular cartilage. High-expression of MMP14, a membrane-associated metalloproteinase required for osteocyte canaliculi formation and matrix remodelling [11], in OA osteocytes could be another factor contributing to SB softening in OA. Although MSC accumulation and atypical differentiation may begin as a consequence of abnormal loading locally, our results show that it is likely to lead to further deleterious impact on the whole joint.

In the present study, we found increased OPG expression in both osteocytes and MSCs from OA bone; however, RANKL levels were unaltered. Immunohistochemical staining in whole femoral head sections revealed strong OPG protein positivity in the trabecular space occupied by the fibrovascular tissue previously implicated in osteophytosis, osteochondral angiogenesis and joint pain [20]. Our findings on OPG association with different types of mesenchymal-lineage cells in OA bone therefore caution against a SB manipulation strategy aimed at bone resorption inhibition in advanced stages of OA.

In summary, given that osteoblast activity is a transient state, our findings document an exaggerated MSC-early osteocyte maturation process in hip OA. They elucidate a cellular mechanism for pathological SB sclerosis and implicate accumulation and preferential osteogenic differentiation of local bone-resident MSCs in human OA pathogenesis. A better understanding of the regional anatomy of the early OA lesions [21], biomechanical and biochemical drivers leading to lesion formation, and their impact on MSC function during disease progression, may lead to novel approaches for preventing disorganized tissue responses in OA. Given the majority of work on human MSCs and osteocytes is still undertaken using cultured cells or cell lines [14], the described methodology would also be relevant for exploring the relationships between native MSCs and osteocytes in other diseases of bone gain or loss, including ankylosing spondylitis and osteoporosis.

Acknowledgements

We thank Mike Shires for his help with processing of histologic samples and advice. We gratefully thank Liz Straszynski and Dr Adam Davidson for their help with cell sorting and Dr Richard Cuthbert for his advice and technical assistance. We further acknowledge the rest of the orthopaedic surgical and nursing teams for their assistance during patient sample collections. All authors were involved in drafting the article or revising it critically for important intellectual content, and all authors approved the final version to be published. E.J. had full access to all of the data in the study and takes responsibility for the integrity of the data and the accuracy of the data analysis. Study conception and design: E.J., D.M., D.C.I., S.M.C. Acquisition of data: D.C.I., S.M.C., T.B., J.A., P.V.G. Analysis and interpretation of data: D.C.I., E.J., D.M., T.B., S.M.C.

Funding: The research is supported by the National Institute for Health Research (NIHR) infrastructure at Leeds. The views expressed are those of the author(s) and not necessarily those of the NHS, the NIHR or the Department of Health.

Disclosure statement: The authors have declared no conflicts of interest.

Supplementary data

Supplementary data are available at *Rheumatology* online.

References

1 Lories RJ, Luyten FP. The bone–cartilage unit in osteoarthritis. Nat Rev Rheumatol 2011;7:43–9.

2 Goldring SR, Goldring MB. Changes in the osteochondral unit during osteoarthritis: structure, function and cartilage-bone crosstalk. Nat Rev Rheumatol 2016;12:632–44.

3 Henrotin Y, Pesesse L, Sanchez C. Subchondral bone and osteoarthritis: biological and cellular aspects. Osteoporos Int 2012;23(Suppl 8):S847–51.

4 Burr DB, Gallant MA. Bone remodelling in osteoarthritis. Nat Rev Rheumatol 2012;8:665–73.

5 Xu L, Hayashi D, Roemer FW, Felson DT, Guermazi A. Magnetic resonance imaging of subchondral bone marrow lesions in association with osteoarthritis. Semin Arthritis Rheum 2012;42:105–18.

6 Prideaux M, Findlay DM, Atkins GJ. Osteocytes: the master cells in bone remodelling. Curr Opin Pharmacol 2016;28:24–30.

7 Martel-Pelletier J, Barr AJ, Cicuttini FM *et al*. Osteoarthritis. Nat Rev Dis Prim 2016;2:16072.

8 Campbell TM, Churchman SM, Gomez A *et al*. Mesenchymal stem cell alterations in bone marrow lesions in patients with hip osteoarthritis. Arthritis Rheumatol 2016;68:1648–59.

9 Muratovic D, Findlay DM, Cicuttini FM *et al*. Bone matrix microdamage and vascular changes characterize bone marrow lesions in the subchondral bone of knee osteoarthritis. Bone 2018;108:193–201.

10 Zhang K, Barragan-Adjemian C, Ye L *et al*. E11/gp38 selective expression in osteocytes: regulation by mechanical strain and role in dendrite elongation. Mol Cell Biol 2006;26:4539–52.

11 Plotkin LI, Bellido T. Osteocytic signalling pathways as therapeutic targets for bone fragility. Nat Rev Endocrinol 2016;12:593–605.

12 Churchman SM, Ponchel F, Boxall SA *et al*. Transcriptional profile of native CD271+ multipotential stromal cells: evidence for multiple fates, with prominent osteogenic and Wnt pathway signaling activity. Arthritis Rheum 2012;64:2632–43.

13 Tormin A, Li O, Brune JC *et al*. CD146 expression on primary nonhematopoietic bone marrow stem cells is correlated with in situ localization. Blood 2011;117:5067–77.

14 Pathak JL, Bakker AD, Luyten FP *et al*. Systemic inflammation affects human osteocyte-specific protein and cytokine expression. Calcif Tissue Int 2016;98:596–608.

15 Jaiprakash A, Prasadam I, Feng JQ *et al*. Phenotypic characterization of osteoarthritic osteocytes from the sclerotic zones: a possible pathological role in subchondral bone sclerosis. Int J Biol Sci 2012;8:406–17.

16 Zhen G, Wen C, Jia X *et al*. Inhibition of TGF-β signaling in mesenchymal stem cells of subchondral bone attenuates osteoarthritis. Nat Med 2013;19:704–12.

17 Jia H, Ma X, Wei Y *et al*. Loading-induced reduction in sclerostin as a mechanism of subchondral bone plate sclerosis in mouse knee joints during late-stage osteoarthritis. Arthritis Rheumatol 2018;70:230–41.

18 Staines KA, Javaheri B, Hohenstein P *et al*. Hypomorphic conditional deletion of E11/Podoplanin reveals a role in osteocyte dendrite elongation. J Cell Physiol 2017;232:3006–19.

19 Staines KA, Ikpegbu E, Javaheri B *et al*. Hypomorphic conditional deletion of E11/podoplanin in the subchondral bone protects against load-induced osteoarthritis. Osteoarthritis Cartilage 2018;26:S61.

20 Suri S, Walsh DA. Osteochondral alterations in osteoarthritis. Bone 2012;51:204–11.

21 Teichtahl AJ, Wang Y, Smith S *et al*. Structural changes of hip osteoarthritis using magnetic resonance imaging. Arthritis Res Ther 2014;16:466.